JOURNAL OF VIROLOGY, Mar. 2007, p. 2128–2137 Vol. 81, No. 5
0022-538X/07/$08.00+0 doi:10.1128/JVI.01494-06

Interaction of Rotavirus Polymerase VP1 with Nonstructural Protein NSP5 Is Stronger than That with NSP2[▽]

F. Arnoldi, M. Campagna, C. Eichwald,† U. Desselberger, and O. R. Burrone*

International Centre for Genetic Engineering and Biotechnology (ICGEB), Padriciano 99, 34012 Trieste, Italy

Received 13 July 2006/Accepted 7 December 2006

Rotavirus morphogenesis starts in intracellular inclusion bodies called viroplasms. RNA replication and packaging are mediated by several viral proteins, of which VP1, the RNA-dependent RNA polymerase, and VP2, the core scaffolding protein, were shown to be sufficient to provide replicase activity in vitro. In vivo, however, viral replication complexes also contain the nonstructural proteins NSP2 and NSP5, which were shown to be essential for replication, to interact with each other, and to form viroplasm-like structures (VLS) when coexpressed in uninfected cells. In order to gain a better understanding of the intermediates formed during viral replication, this work focused on the interactions of NSP5 with VP1, VP2, and NSP2. We demonstrated a strong interaction of VP1 with NSP5 but only a weak one with NSP2 in cotransfected cells in the absence of other viral proteins or viral RNA. By contrast, we failed to coimmunoprecipitate VP2 with anti-NSP5 antibodies or NSP5 with anti-VP2 antibodies. We constructed a tagged form of VP1, which was found to colocalize in viroplasms and in VLS formed by NSP5 and NSP2. The tagged VP1 was able to replace VP1 structurally by being incorporated into progeny viral particles. When applying anti-tag-VP1 or anti-NSP5 antibodies, coimmunoprecipitation of tagged VP1 with NSP5 was found. Using deletion mutants of NSP5 or different fragments of NSP5 fused to enhanced green fluorescent protein, we identified the 48 C-terminal amino acids as the region essential for interaction with VP1.

Rotavirus is a major etiologic agent of severe gastroenteritis in infants and young children worldwide (20, 21, 33). The virion (defined as a triple-layered particle [TLP]) contains a genome consisting of 11 segments of double-stranded RNA (dsRNA) and is made up of three concentric layers of proteins: the outer layer consists of the two proteins VP7 and VP4, the intermediate layer of VP6, and the internal (core) layer of VP2, with VP1 and VP3 attached at its inside as minor components (29, 41). After entry into the host cell, the virion loses the outer layer to become a double-layered particle (DLP), which is active in transcription of viral mRNAs from the dsRNA genome. The viral RNA-dependent RNA polymerase (RdRp) acts as both the transcriptase and the replicase. Several lines of evidence indicate that VP1 is the viral RdRp: (i) VP1 contains sequence motifs that are shared by RdRps of other RNA viruses (31); (ii) VP1 has NTP-binding activity and, when cross-linked with the nucleotide analog 8-azido-ATP, inhibits RNA transcription (50); (iii) VP1 specifically recognizes the 3′ end of viral mRNAs (35); and (iv) recombinant VP1 can direct template-dependent minus-strand synthesis in vitro in the presence of VP2 (37, 54).

Despite partial characterization of rotavirus replication intermediates (3, 19, 36, 37, 54), molecular details of viral genome replication and of the different steps of viral morphogenesis still remain to be elucidated. It has been shown that VP1 and VP2, the scaffolding protein of viral cores, are minimally necessary but also sufficient to provide replicase activity in vitro (37, 54). In vivo early viral replicase complexes in addition contain nonstructural proteins associated with the structural proteins (3, 19, 36). The work of several research groups has demonstrated that the two nonstructural proteins NSP2 and NSP5 are essential to promote replication during natural infection (8, 30, 44, 51) and accumulate together with other structural proteins (VP1, VP2, VP3, and VP6) in spherical cytoplasmic structures, called viroplasms, that appear early after infection and are sites of viral replication and packaging (38, 39).

NSP2 binds single-stranded RNA in a nonspecific manner and self-assembles into stable octamers that have Mg^{2+}-dependent NTPase and helix destabilizing activities (43, 46, 47). NSP5 is an *O*-GlcNAc-glycosylated (22) acidic phosphoprotein with a high number of lysines at its C terminus (2, 6, 11, 40, 53). It self-assembles into dimers (48) and also binds RNA nonspecifically (52). NSP2 and NSP5 are known to interact with each other. This interaction was described in vitro with purified proteins (24) and in vivo for both infected cells (1, 12, 40) and uninfected, cotransfected cells, where coexpression of the two proteins leads to up-regulation of NSP5 hyperphosphorylation and to the formation of viroplasm-like structures (VLS) (1, 17). The signals promoting the formation of VLS seem to be embedded in the C- and N-terminal regions of NSP5 (12, 32). NSP5 also has been shown to interact with VP1, but this interaction has so far been reported only for infected cells (1). An interaction between NSP2 and VP1 has also been described following in vitro chemical cross-linking of extracts from infected cells (25).

In order to gain a more detailed understanding of the intermediates formed during genome replication, we focused

* Corresponding author. Mailing address: International Centre for Genetic Engineering and Biotechnology (ICGEB), Padriciano 99, 34012 Trieste, Italy. Phone: 39-040-3757314. Fax: 39-040-226555. E-mail: burrone@icgeb.org.

† Present address: Department of Microbiology and Molecular Genetics, Harvard Medical School, 200 Longwood Ave., Boston, MA 02115.

▽ Published ahead of print on 20 December 2006.

our work on the interaction of NSP5 with VP1, VP2, and NSP2.

MATERIALS AND METHODS

Cells, viruses, radiolabeling with [^{35}S]methionine, and transient transfections. MA104 cells were grown as monolayers in Dulbecco's modified Eagle's medium containing 10% fetal calf serum, 2 mM L-glutamine, and 50 mg/ml gentamicin (Gibco BRL). The simian SA11 (G3, P6[1]) and bovine RF (G6, P6[1]) strains of rotavirus were propagated in MA104 cells as described previously (15, 23). Labeling of cells with [^{35}S]methionine was performed as described by Afrikanova et al. (2). For transfection experiments, confluent monolayers of MA104 cells in six-well plates (Falcon) were infected with T7-recombinant vaccinia virus (strain vTF7.3) (18) and 1 h later transfected with a maximum total of 3 μg/well of plasmid DNA (1 μg of each plasmid in cotransfections) using 5 μl of Lipofectamine 2000 (Gibco BRL) and following the manufacturer's instructions. Infection with T7-recombinant vaccinia virus was used to increase the expression level of proteins encoded by the transfected plasmids. Transfected cells were harvested at 18 h posttransfection. Cellular extracts were prepared in 100 μl of TNN lysis buffer (100 mM Tris-HCl, pH 8, 250 mM NaCl, 0.5% NP-40) at 4°C and were centrifuged at 15,800 × *g* for 5 min. Usually, 10 μl of supernatants were used in polyacrylamide gel electrophoresis (PAGE) and Western immunoblot analyses, and 40 to 80 μl were used for immunoprecipitation experiments. The pellets were washed three times with phosphate-buffered saline (PBS) (170 mM NaCl, 10 mM phosphate, 3 mM KCl, pH 7.4) and resuspended in 20 μl of loading buffer for PAGE and Western blot analyses.

Purification of virus particles. Confluent monolayers of MA104 cells in six six-well plates were infected with T7-recombinant vaccinia virus (strain vTF7.3) and 1 h later transfected with pcDNA3-SV5-VP1 (2 μg of DNA per well), using Lipofectamine 2000 (5 μl per well; Gibco BRL). Six hours posttransfection, cells were washed with serum-free medium and infected with the bovine RF rotavirus strain at a multiplicity of infection of 3. Viral particles were purified from cell cultures after harvest at about 20 h postinfection, when almost complete cytopathic effect had been reached. Virus was pelleted by ultracentrifugation and the pellets extracted with Freon (trichlorotrifluoroethane; Sigma) and banded by equilibrium ultracentrifugation in CsCl gradient, essentially as described by Patton et al. (34). This allowed the obtaining of three well-separated gradient bands containing empty particles (EPs), TLPs, and DLPs. Empty particle, TLP, and DLP suspensions were diluted in 20 mM piperazine-*N*,*N*′-bis(2-ethanesulfonic acid) buffer (pH 6.6) containing 10 mM $CaCl_2$ and pelleted by ultracentrifugation at 110,000 × *g* for 1 h in a Beckman ultracentrifuge using an SW55 rotor. The pellets containing the different viral particles were resuspended in 35 μl of water and used in sodium dodecyl sulfate (SDS)-PAGE and Western immunoblot analyses.

EDTA treatment of purified TLPs. Pellets derived from ultracentrifugation of CsCl-purified TLP suspensions were resuspended in 60 μl of piperazine-*N*,*N*′-bis(2-ethanesulfonic acid) buffer (pH 6.6) containing 0.5 mM $CaCl_2$ and treated with 5 mM EDTA in PBS for 30 min at 37°C in modification of the procedure of Estes et al. (16). The resulting particles were pelleted by ultracentrifugation and analyzed by SDS-PAGE and Western blotting.

Construction of plasmids. pcDNA3-NSP5 and pcDNA3-NSP2 were obtained as described previously (17). The NSP5 gene was derived from the OSU rotavirus strain (GenBank accession number D00474) and the NSP2 gene from the SA11 strain (accession number L04532). The VP1 and VP2 genes (accession numbers X16830 and L33364, respectively) were cloned from SA11 rotavirus-infected cells: viral RNA was extracted from 500 μl of cell supernatant after complete cytopathic effect had been reached. The cDNA was obtained by reverse transcription, using random hexamers (Sigma Genosys) and murine leukemia virus reverse transcriptase (Applied Biosystems). Subsequently, the cDNA spanning the open reading frame (ORF) of VP1 was amplified in two portions by PCR: the VP1/I amplicon reached from nucleotide (nt) 19 (first nucleotide of the start codon) to nt 1322 and VP1/II from nt 1231 to nt 3285 (last nucleotide of the stop codon). In the region present in both amplified fragments (nt 1231 to 1322), an NsiI site was used to ligate the two VP1 fragments in order to obtain the cDNA of the complete ORF. The primers used to amplify VP1/I were the following (with the portions of sequence derived from the VP1 gene indicated in capital letters): 5′-tagggtaccATGGGGAAGTACAATCTAATC-3′ (the start codon is underlined) and 5′-atggaattcggCGTGTATCTTTCGTTAGC-3′. The primers used to amplify the VP1/II were 5′-tagggtaccTCAAGGCAGCTAAAGTTTGG-3′ and 5′-ccgctcgagCTAATCTTGAAAGAAGTTCGC-3′ (the stop anticodon is underlined). The ligation product was cloned into the pGEM-T Easy vector (Promega) and sequenced (MWG-Biotech, Ebersberg, Germany). The VP1/I amplicon was subcloned into the NcoI- and EcoRI-digested Pet23d vector (Novagen) containing a histidine tag to express the protein in bacteria, while the complete VP1 cDNA was subcloned into the KpnI- and XhoI-digested pcDNA3 vector (Invitrogen) for expression in mammalian cells. Similarly, the cDNA spanning the ORF of VP2 was amplified in two portions by PCR. The VP2/I amplicon was obtained using the following primers (with the portions of sequence derived from the VP2 gene indicated in capital letters): 5′-tatcaggtac cATGGCGTATCGAAAACGTGGA-3′ (the start codon is underlined) and 5′-ttgtcaaagcttCCAATTGCAAATCTTG-3′. The VP2/II amplicon was obtained using primers 5′-aattggaagcttTGACAATACAATCAGAGA-3′ and 5′-taataa gatatcTTACAGTTCGTTCATGAT-3′ (the stop anticodon is underlined). The VP2/I and VP2/II amplicons were cloned into pGEM-T Easy vectors and sequenced. To obtain the complete VP2 cDNA, the VP2/II amplicon was cut with the HindIII and EcoRV restriction enzymes and inserted downstream of VP2/I in the pGEM-T Easy-VP2/I vector, previously cut with HindIII and EcoRI, followed by end filling with the Klenow fragment. The complete VP2 cDNA was inserted into the pcDNA3 vector following digestion with the KpnI and NotI restriction enzymes. The pcDNA3-SV5-VP1 plasmid was obtained by inserting the SV5 tag (45) at the N terminus of VP1. The following oligonucleotides were annealed and inserted in the HindIII- and KpnI-digested pcDNA3-VP1 vector: 5′-AGCTTGTACCATGGGCAAACCAATCCCAAACCCACTGCTGGGTCTGGATGGTAC-3′ and 5′-CATCCAGACCCAGCAGTGGGTTTGGGATTGGTTTGCCCATGGTACA-3′. The SV5 peptide coding sequence is underlined.

The constructs coding for the deletion mutants of NSP5, pT_7v-Δ1 (termed Δ1), pT_7v-ΔT (ΔT), pT_7v-Δ4ΔT (Δ4ΔT), and pT_7v-ΔC48 (ΔC48), and the pT_7v-(dom1EGFP4T) (1E4T), pT_7v-(EGFP-4T) (E4T), and pT_7v-(dom1EGFP) (1E) vectors have been described previously (1, 12, 13, 17).

Production of antibodies. Anti-NSP5 and anti-NSP2 sera were produced by immunization of guinea pigs and anti-VP7 serum by immunization of rabbits as described previously (22). Serum anti-VP1 was produced by immunization of guinea pigs with the histidine-tagged VP1/I protein fragment (amino acids 1 to 435). The protein was produced in the *Escherichia coli* BL21 strain. Cultures were induced with 3 mM isopropyl-beta-D-thiogalactopyranoside for 3 to 4 h at 37°C. Bacteria were centrifuged, and the pellet was washed with ice-cold PBS and resuspended in 1.5% laurylsarcosin-PBS supplemented with 0.1 μg/μl lysozyme, 1× CLAP cocktail (chymostatin, leupeptin, aprotinin, and pepstatin; 10 μg/ml each), and 5 mM dithiothreitol for sonication (six times, 10 s, using the Soniprep 150 instrument with the 9.5-mm probe tuned at 23 kHz). The supernatant was supplemented with 1% Triton X-100 in PBS (pH 7.2) and with Ni-nitrilotriacetic acid His-Bind resin (Novagen) equilibrated in 20 mM imidazole in PBS. After rolling for 1 h at 4°C, the sample was centrifuged at 1,000 × *g* for 5 min at 4°C, and the resin was washed with 10 volumes of 35 mM imidazole in PBS. Elution was performed with two volumes of imidazole, 250 mM. Guinea pigs were injected intraperitoneally with 100 μg of protein and boosted 3 times (100 μg every 15 days intraperitoneally). Sera of the immunized guinea pigs were tested by Western blotting on extracts of rotavirus-infected and uninfected cells.

Chemical DSP cross-linking. Dithiobis(succinimidylpropionate) (DSP) was purchased from Pierce. Monolayers of transfected cells were washed twice with PBS, overlaid with 1.5 ml PBS containing 600 μM DSP, and incubated at 4°C for 30 min. After removal of the reactant solution, the reaction was quenched twice

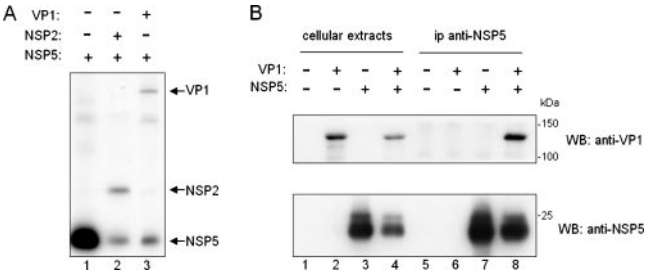

FIG. 1. Coimmunoprecipitation of VP1 and NSP5. (A) Immunoprecipitation (ip) with anti-NSP5 serum of DSP-cross-linked extracts of [^{35}S]methionine-labeled cells transiently transfected with the indicated genes. (B) Western blot analysis of DSP-cross-linked cellular extracts (lanes 1 to 4) or immunoprecipitates (lanes 5 to 8) derived from cells cotransfected with VP1 and NSP5. After separation by PAGE and Western blotting, the upper and lower parts of the blot were reacted with specific anti-VP1 or anti-NSP5 antibodies, respectively.

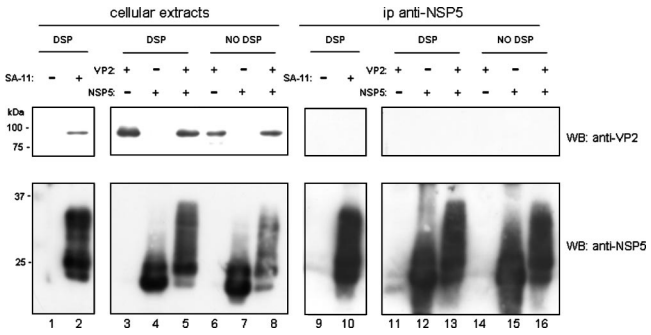

FIG. 2. Analysis of coimmunoprecipitation of VP2 with NSP5. Western blot analysis of cellular extracts (lanes 1 to 8, DSP cross-linked in lanes 1 to 5 and non-cross-linked in lanes 6 to 8) or immunoprecipitates (lanes 9 to 16, DSP cross-linked in lanes 9 to 13 and non-cross-linked in lanes 14 to 16) derived from cells infected with rotavirus (lanes 1 and 2, 9 and 10) or cotransfected with VP2 and NSP5 (lanes 3 to 8, 11 to 16). After separation by PAGE and Western blotting, the upper and lower parts of the blots were reacted with specific anti-VP2 or anti-NSP5 antibodies, respectively.

with 2 ml Tris-buffered saline (40 mM Tris-HCl [pH 8], 150 mM NaCl) for 3 min at 4°C. Cellular extracts were prepared in 100 μl TNN as described above.

RNase treatment of protein complexes. For RNase treatment, cellular extracts were prepared by applying a lysis buffer consisting of PBS diluted 1:10 (to reduce salt concentration) and containing NP-40 (0.5%). Subsequently, 70 μl of these extracts were treated with 10 units of RNase One (Promega) in 8 μl of reaction buffer (provided by Promega) for 10 min at 37°C. Afterwards, 1 μl undiluted antibody, 50 μl of 50% protein A-Sepharose CL-4B beads in TNN buffer, 1 μl of 100 mM phenylmethylsulfonyl fluoride, and TNN were added to obtain a final volume of 500 μl for immunoprecipitation.

Immunoprecipitation, PAGE, and Western immunoblot analysis. Cellular extracts (usually 4/5 of the total extract, i.e., approximately 80 μl) were immunoprecipitated overnight at 4°C after addition of 1 μl of undiluted antibody, 1 μl of 100 mM phenylmethylsulfonyl fluoride, 50 μl of 50% protein A-Sepharose CL-4B beads (Amersham Biosciences) in TNN buffer, and 20 μl of TNN buffer. Beads were then washed four times with TNN buffer and once with PBS and resuspended in 20 μl of loading buffer. Sample components were separated by SDS-PAGE (28) (using the Precision Plus Protein Standards molecular markers; Bio-Rad) and after electrophoresis transferred to polyvinylidene difluoride membranes (Millipore) (49). The membranes were incubated with the following antibodies: anti-NSP5 guinea pig serum (1:8,000), anti-NSP2 guinea pig serum (1:1,000), anti-VP1 guinea pig serum (1:1,000), anti-VP7 rabbit serum (1:1,000), anti-VP2 guinea pig serum (1:2,000), monoclonal antibody anti-SV5 (1:10,000), and peroxidase-conjugated goat anti-guinea pig, goat anti-mouse, and goat anti-rabbit secondary antibodies (KPL) (1:5,000 each). Signals were detected by using the enhanced chemiluminescence system (Pierce).

Immunofluorescence microscopy. Immunofluorescence experiments were performed as described previously (13) with the following antibody dilutions: anti-NSP5 guinea pig serum, 1:300 for transfected cells and 1:3,000 for infected cells; anti-NSP2 guinea pig serum, 1:100; anti-SV5 monoclonal antibody, 1:300; rhodamine isothiocyanate-conjugated goat anti-guinea pig (KPL), 1:200; and fluorescein isothiocyanate-conjugated goat anti-mouse secondary antibodies (Jackson ImmunoResearch), 1:200. Samples were analyzed by confocal microscopy (Axiovert; Carl Zeiss).

RESULTS

VP1 but not VP2 coimmunoprecipitates with NSP5. Interaction between NSP5 and VP1 was first observed by coimmunoprecipitation with anti-NSP5 antibody in extracts from cells transiently transfected, labeled with [^{35}S]methionine, and in vivo cross-linked with DSP (Fig. 1A, lane 3). DSP is a reagent with two reactive groups separated by a spacer of 12-Å length, able to permeate cell membranes and to cross-link proteins interacting inside the cell through their amino groups. In addition, a disulfide bridge within this spacer allows the separation of the components of the cross-linked complex under reducing conditions. Coimmunoprecipitation of NSP2 with NSP5, which are well known to interact (1), served as an internal control (Fig. 1A, lane 2). A similar result was obtained

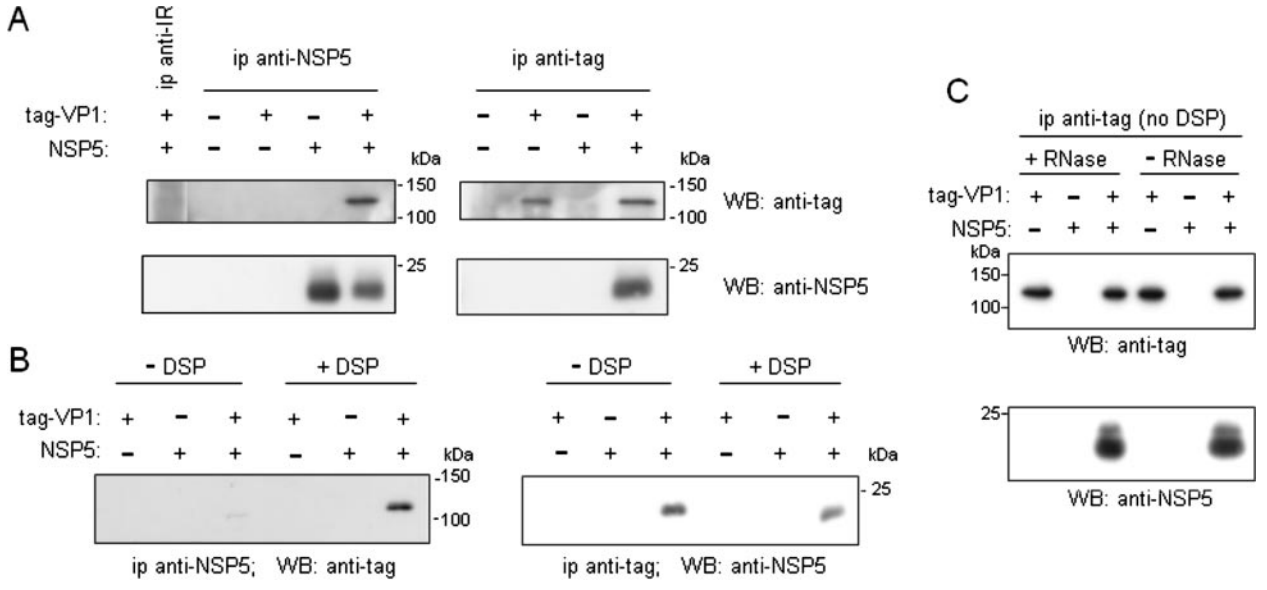

FIG. 3. Coimmunoprecipitation of NSP5 and tagged VP1. (A) Western blot of immunoprecipitates (ip) of DSP-cross-linked extracts from MA104 cells cotransfected with NSP5 and a VP1 derivative, N-terminally modified with the SV5 tag. Immunoprecipitates were obtained with an anti-NSP5 serum (anti-NSP5) and the anti-SV5 monoclonal antibody (anti-tag) and upper and lower parts of the blots developed with either of them, as described in legend to Fig. 1. (B) Western blot of immunoprecipitates obtained with anti-NSP5 or anti-tag antibody from both extracts of non-cross-linked or DSP-cross-linked cells and developed with the indicated antibodies. (C) Western blot of immunoprecipitates obtained with anti-NSP5 from extracts of non-DSP-cross-linked cells, treated with RNase or not treated.

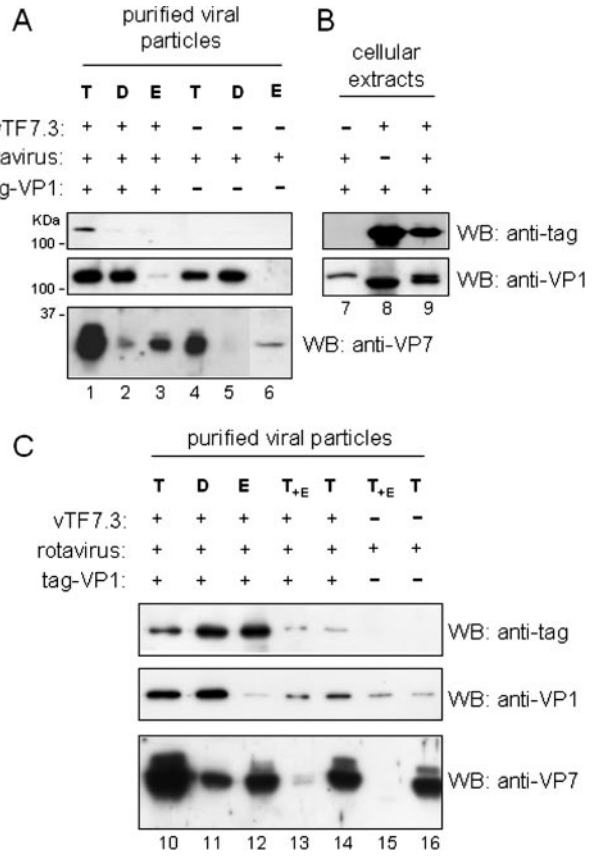

FIG. 4. Packaging of tag-VP1. Rotavirus particles, obtained from infected cells expressing tag-VP1 and purified by CsCl gradient ultracentrifugation, were analyzed by Western blotting with anti-tag, anti-VP1, or anti-VP7 antibody, as indicated. vTF7.3 was used to drive expression of tag-VP1. (A) Rotavirus particles (T, TLPs; D, DLPs; E, EPs) obtained from cells transfected with tag-VP1 (lanes 1 to 3) or nontransfected (lanes 4 to 6) were analyzed by Western blotting as indicated. (B) Western blot of total cellular extracts. Lane 9 corresponds to the conditions under which viral particles shown in lanes 1 to 3 were obtained. Of note, tag-VP1 (SA11 strain; lane 8) migrated faster than the untagged VP1 (RF strain; lane 7). (C) Western blot with anti-tag, anti-VP1, and anti-VP7 antibodies of TLPs, DLPs, and EPs obtained as for panel A (lanes 10 to 12, respectively). Tag-VP1 TLPs and control TLPs were treated with EDTA as described (T_{+E}; lanes 13 and 15, respectively) or mock treated (lanes 14 and 16, respectively). The traces of VP7 in the DLP preparations (lanes 2 and 11) are probably due to contamination with small amounts of TLPs.

with MA104 cells transfected with plasmids expressing the NSP5 and VP1 genes, immunoprecipitated with anti-NSP5 antibody, and tested by Western blotting with an anti-VP1 serum (Fig. 1B).

By contrast, in cells infected with SA-11 rotavirus or cotransfected with plasmids expressing NSP5 and VP2, no coimmunoprecipitation was observed. While both NSP5 and VP2 were well expressed, VP2 was not coimmunoprecipitated with anti-NSP5 (Fig. 2, lanes 13 and 16), regardless of whether cells had previously been treated or not treated with DSP. Similarly, anti-VP2 antibodies did not coimmunoprecipitate NSP5 (data not shown). In addition, coimmunoprecipitation of VP2 with anti-NSP5 from extracts of virus-infected cells was not observed (Fig. 2, lane 10), either, in agreement with previous

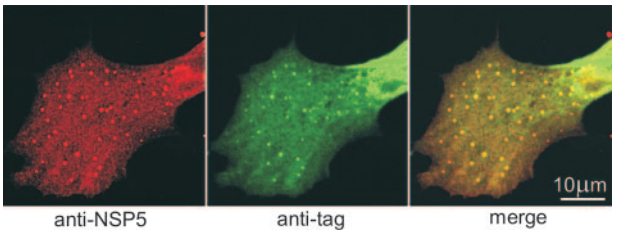

FIG. 5. Colocalization of tag-VP1 in viroplasms. Confocal immunofluorescence of tag-VP1 (green) and NSP5 (red) in MA104 cells transfected with the tag-VP1-expressing plasmid and infected with SA-11 rotavirus. The individual and merged patterns are shown.

reports (1). In a novel finding, a remarkable increase in NSP5 hyperphosphorylation was apparent in cells coexpressing VP2 (Fig. 2, lanes 5, 8, 13, and 16).

In order to further investigate the interaction between NSP5 and VP1 and because the anti-VP1 antibody did not react in immunoprecipitations nor in immunofluorescence, we used a VP1 derivative (tag-VP1) containing the 11-amino-acid-long SV5 tag (45) at its N terminus, for which a potent monoclonal antibody (anti-tag) was available. Extracts from cells cotransfected with NSP5 and tag-VP1 vectors (pcDNA3-NSP5 and pcDNA3-SV5VP1, respectively) were immunoprecipitated with either anti-NSP5 or the anti-tag antibody, and the immunoprecipitates were analyzed by Western blotting with both antibodies. It was found that NSP5 and tag-VP1 coimmunoprecipitated in both cases (Fig. 3A). The comparison between assays using cross-linked or non-cross-linked cellular extracts revealed that DSP cross-linking was needed only for immunoprecipitations with anti-NSP5 antibody but not with the anti-tag antibody (Fig. 3B).

To test whether cellular RNA mediates interaction between NSP5 and VP1, cellular extracts from non-cross-linked cells were treated or not treated with RNase One (RNase) before immunoprecipitation and Western blot analysis. Figure 3C shows that RNase treatment did not change the ability of anti-tag antibody to coimmunoprecipitate NSP5. We also examined UV treatment of cells as an alternative method that cross-links nucleic acids. It has been previously observed that UV treatment of rotavirus-infected cells visualized only the interaction between NSP5 and NSP2, while with DSP cross-linking, VP1 was also coimmunoprecipitated (1). In agreement with this finding and with the lack of an effect of RNase digestion, UV treatment of cells coexpressing VP1 and NSP5 did not result in coimmunoprecipitation of tag-VP1 with anti-NSP5 antibody (data not shown).

Tag-VP1 can act as a structural replacement of VP1. To ensure the validity of using tag-VP1 instead of VP1, the behavior of the tagged protein in the course of viral infection was investigated. We tested whether the transfected tag-VP1 was incorporated into particles of viral progeny in MA104 cells infected with vTF7.3 recombinant vaccinia virus, transfected with a plasmid encoding tag-VP1, and 6 hours later superinfected with the rotavirus RF strain. Twenty hours after rotavirus infection, viral progeny particles were concentrated by sedimentation and purified by CsCl gradient ultracentrifugation. Fractions of gradients containing the visible bands of EPs (density, 1.30 g/ml), TLPs (1.36 g/ml), and DLPs (1.38 g/ml)

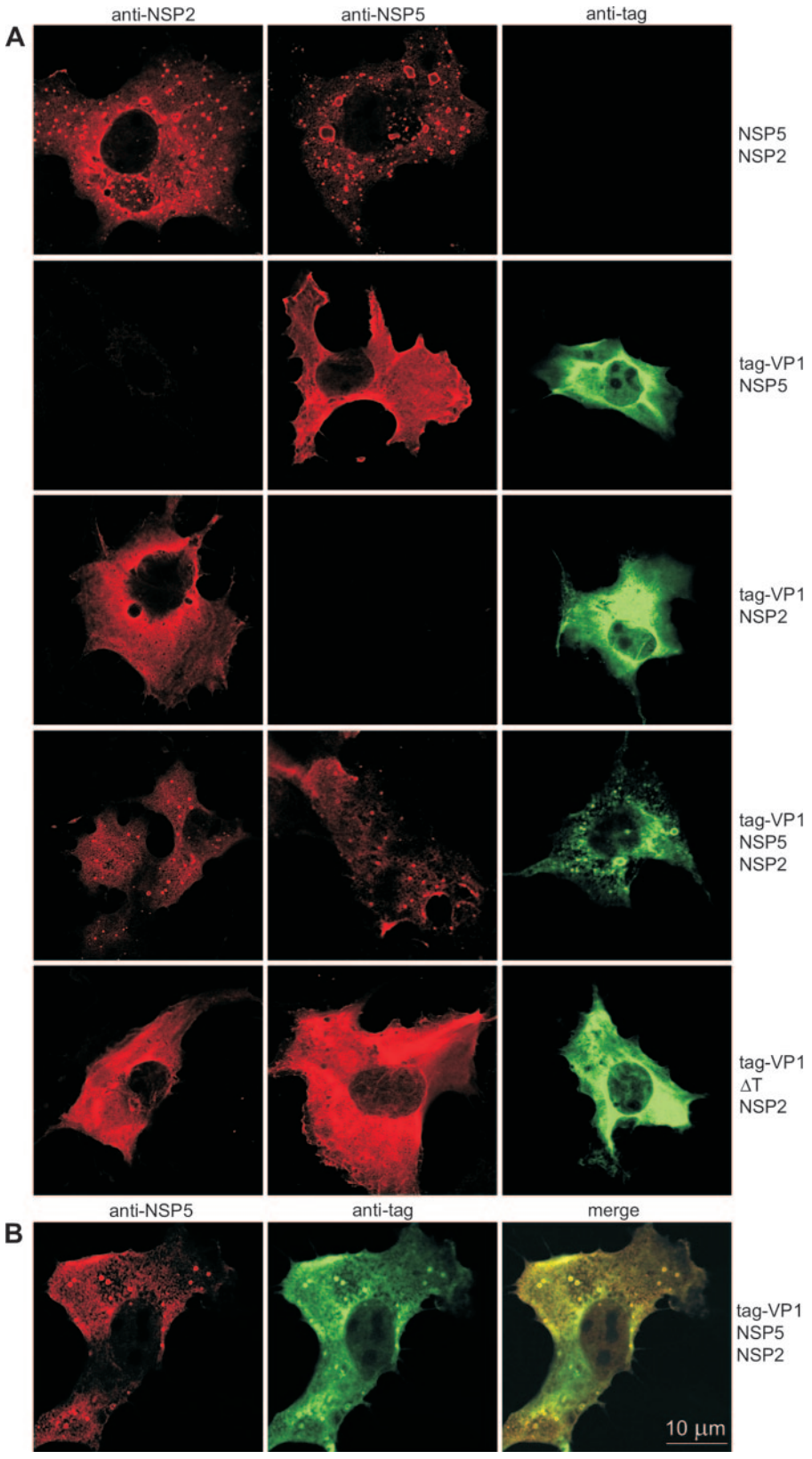

FIG. 6. Localization of tag-VP1 in VLS. (A) Immunofluorescence of tag-VP1 (green), NSP2 (red), and NSP5 (red) in cells cotransfected with and expressing the indicated genes. (B) Colocalization of tag-VP1 and NSP5 in VLS formed in cells coexpressing NSP5, NSP2, and tag-VP1, as shown by confocal microscopy with anti-NSP5 (red) and anti-tag (green).

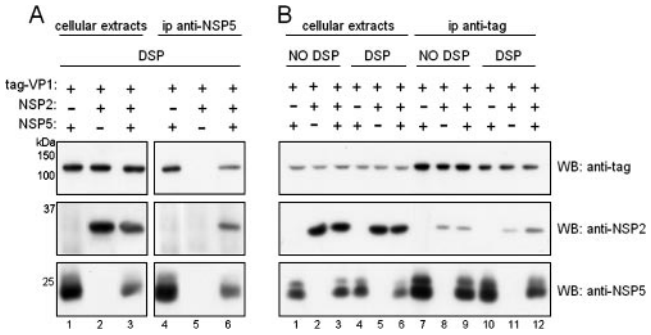

FIG. 7. Coimmunoprecipitation of NSP2, NSP5, and tag-VP1. (A) Western blot of cellular extracts (lanes 1 to 3) or anti-NSP5 immunoprecipitates (lanes 4 to 6) derived from cells transfected with NSP2, NSP5, and tag-VP1 and DSP cross-linked. (B) Western blot of cellular extracts (lanes 1 to 6) or anti-tag immunoprecipitates (lanes 7 to 12) derived from cells transfected with NSP2, NSP5, and tag-VP1, DSP cross-linked (lanes 4 to 6, 10 to 12) or non-cross-linked (lanes 1 to 3, 7 to 9). Upper, middle, and lower parts of the blots were cut and reacted with anti-tag, anti-NSP2, or anti-NSP5 antibodies, respectively.

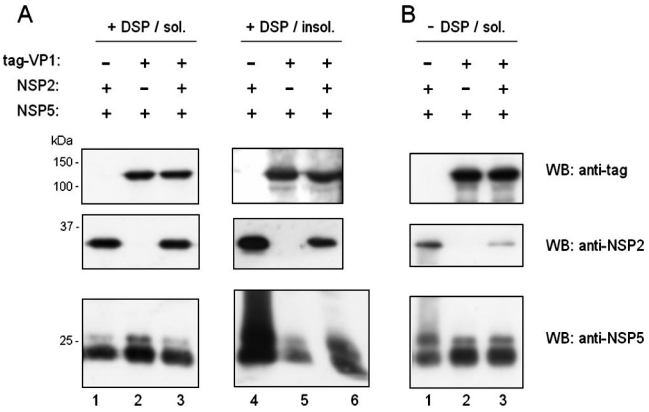

FIG. 8. Effects of DSP cross-linking and tag-VP1 on NSP5 hyperphosphorylation. (A) Western blot (WB) analysis of the soluble (sol.) (left panel, lanes 1 to 3) and insoluble (insol.) (right panel, lanes 4 to 6) fractions derived from extracts of DSP-cross-linked cells transfected with and expressing the genes, as indicated. (B) Western blot of the soluble fractions of non-cross-linked cells. Upper, middle, and lower parts of the blots were cut and reacted with anti-tag, anti-NSP2, or anti-NSP5 antibodies, respectively.

(14) were analyzed by Western blotting with anti-tag and anti-VP1 antibodies and with anti-VP7 as a control. Cellular extracts of transfected cells in the presence or in the absence of vaccinia virus and/or rotavirus were tested in the same way. Tag-VP1 was found to be incorporated into viral particles in an unambiguous and reproducible fashion in several experiments (Fig. 4). These experiments showed some variability in the relative amounts of tag-VP1 found in TLPs, DLPs, and EPs. In some experiments, tag-VP1 was incorporated mostly into TLPs, and only faint tag-VP1 bands were observed in DLPs and EPs (Fig. 4A); in others, tag-VP1 was preferentially present in DLPs (Fig. 4C). To rule out nonspecific trapping of tag-VP1 in the outer shell of TLPs, we treated purified TLPs with EDTA to remove the outer layer (16). The treatment did not release tag-VP1 (Fig. 4C), indicating that tag-VP1 was genuinely incorporated into DLPs. This conclusion was strengthened by comparison of the relative amounts of VP1 (anti-VP1) and tag-VP1 (anti-tag) in lanes 10, 13, and 14, which showed similar ratios. The difference in PAGE mobility between tag-VP1 and wild-type VP1 (Fig. 4B) was caused by them being derived from two different rotavirus strains (tag-VP1, SA11 strain; wild-type VP1, RF strain).

Tag-VP1 colocalizes with NSP5 in viroplasms and in viroplasm-like structures. In virus-infected cells, NSP5 and VP1, as well as NSP2, colocalize in the cytoplasmic viroplasms. We now found that tag-VP1 also localizes in viroplasms. As shown in Fig. 5, confocal microscopy with different fluorescence labels for the NSP5 and tag-VP1 signals revealed that part of tag-VP1 colocalized with NSP5 in the viroplasms of rotavirus-infected cells. When tag-VP1 was coexpressed in uninfected cells, either with NSP5 or with NSP2 in the absence of any other rotavirus protein, a diffuse cytoplasmic distribution for each individual protein was observed (Fig. 6A, horizontal rows 2 to 3). By contrast, when NSP5 and NSP2 were both present, a substantial part of tag-VP1 was found to localize in the characteristic viroplasm-like structures (VLS), which are formed by the two nonstructural proteins (17) (Fig. 6A, row 4, and Fig. 6B). This was further confirmed by cotransfecting NSP2 with a mutant of NSP5 lacking the 18-amino-acid C-terminal tail region (ΔT), which had previously been demonstrated to be unable to form VLS (17). As expected, all three proteins showed a diffuse distribution (Fig. 6A, row 5). While VLS of cells containing tag-VP1 appear to be smaller and less numerous than VLS formed only by NSP5 and NSP2, they still retain the typical ring appearance (Fig. 6A, row 4).

VP1 interacts more strongly with NSP5 than with NSP2. As previously mentioned, NSP5, NSP2, and VP1 can be coimmunoprecipitated from virus-infected cells (1). Similarly, all three proteins were coimmunoprecipitated by anti-NSP5 antibody from extracts of cells coexpressing them in the absence of other viral proteins (Fig. 7A, lane 6). As previously reported, anti-NSP2 antibody did not pull down either NSP5 (1) or tag-VP1 (data not shown).

We then compared the ability of anti-tag antibody to coimmunoprecipitate NSP5 and/or NSP2 from extracts of DSP-cross-linked and non-cross-linked cells. Anti-tag antibody was able to coimmunoprecipitate NSP5 and NSP2 when tag-VP1 was coexpressed with either of them (Fig. 7B, lanes 7 and 8 and lanes 10 and 11) or with both (Fig. 7B, lanes 9 and 12). It is apparent that coimmunoprecipitation of NSP5 is much more efficient than coimmunoprecipitation of NSP2. In fact, although the input of cellular extracts used for immunoprecipitations represented four times as much as that used for the analysis of cellular extracts (Fig. 7B, lanes 1 to 6), only a small fraction of NSP2 was recovered from the immunoprecipitates, whereas the amount of NSP5 recovered was significantly larger. In several experiments we observed that from DSP-cross-linked extracts the amount of NSP2 coimmunoprecipitated with VP1 was larger when NSP5 was present (Fig. 7B, lanes 11 and 12). Altogether these data indicate that in contrast to NSP5, NSP2 interacts weakly with VP1.

Since NSP5 becomes hyperphosphorylated in the presence of NSP2 (1), we expected to find the hyperphosphorylated forms of NSP5 in the immunoprecipitates. However, after DSP cross-linking, these forms were found only in the insoluble fraction (Fig. 8A, lane 4) and were surprisingly absent when tag-VP1

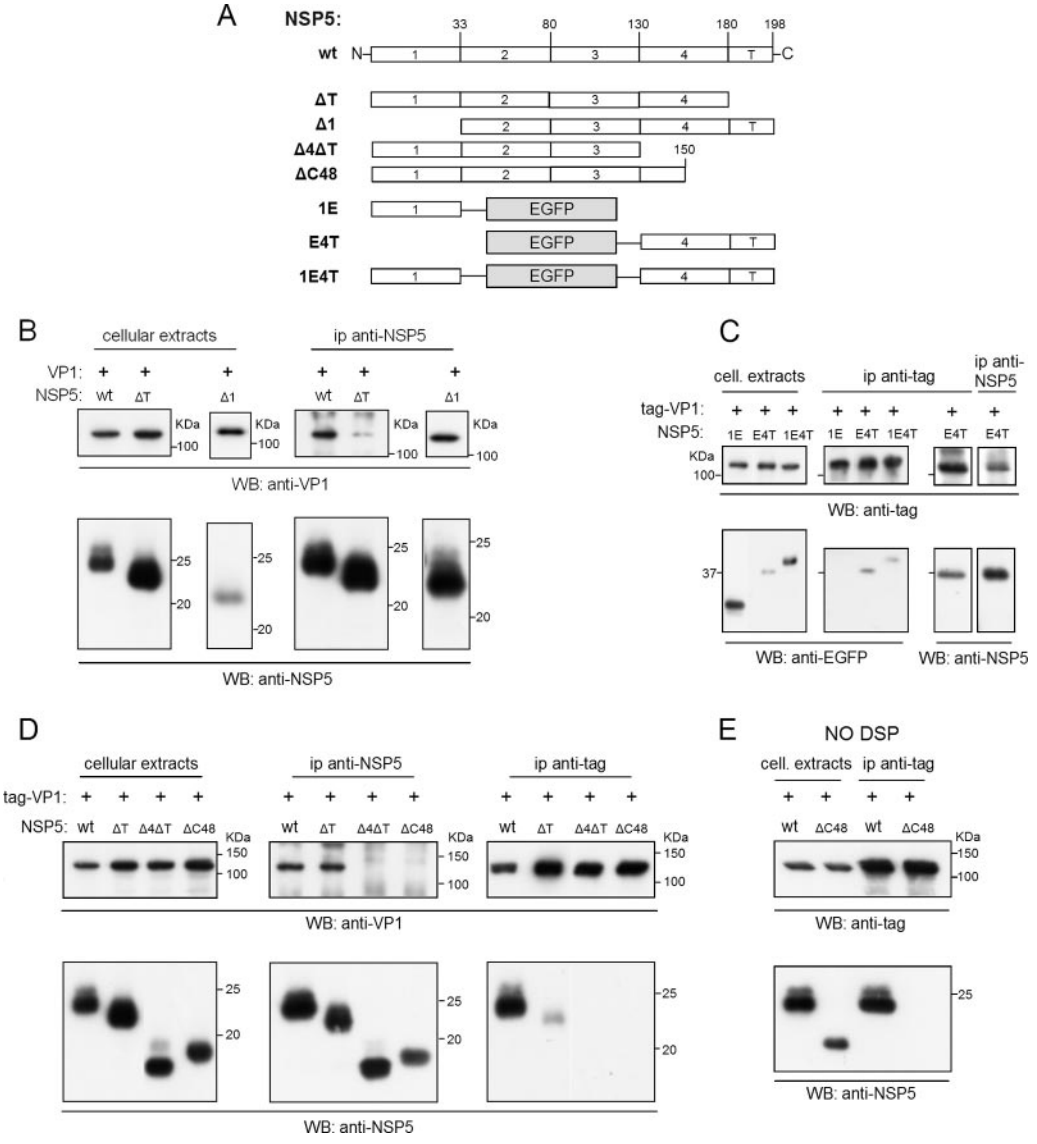

FIG. 9. Interaction of VP1 with NSP5 mutants. (A) Diagram of NSP5 mutant constructs used. (B to D) Western blots of DSP-cross-linked cellular extracts or immunoprecipitates of cells cotransfected with wild-type (wt) VP1 (B) or tag-VP1 (C and D) and NSP5 or NSP5 mutants, as indicated. (E) Western blot of non-DSP-cross-linked cellular extracts or immunoprecipitates derived from cells cotransfected with tag-VP1 and either wt NSP5 or the mutant ΔC48.

and NSP2 were present (Fig. 8A, lane 6). Furthermore, even in extracts not cross-linked with DSP, the relative hyperphosphorylation of NSP5 in cells coexpressing tag-VP1 and NSP2 was clearly impaired (Fig. 8B, compare lane 3 to lane 1), suggesting that VP1 inhibits the up-regulation of NSP2-mediated NSP5 hyperphosphorylation.

The NSP5 C-terminal 48 amino acids are essential for interaction with VP1. To map the region of NSP5 essential for the interaction with VP1, we first performed coimmunoprecipitation assays using extracts of cells cotransfected with plasmids encoding tag-VP1 and either of two deletion mutants of NSP5, lacking the first 33 N-terminal amino acids (Δ1) or the 18-amino-acid-long C-terminal tail (ΔT) (Fig. 9A). As shown in Fig. 9B, anti-NSP5 coimmunoprecipitated VP1 when coexpressed with Δ1, whereas only a small amount of VP1 was obtained when VP1 was coexpressed with ΔT. In conclusion, these data indicate that the interaction with VP1 did not involve the N-terminal region of NSP5 and was substantially reduced by the removal of the last 18 amino acids from the C terminus. This observation was strengthened by carrying out cotransfections of the tag-VP1 construct with the same two mutants followed by immunoprecipitations with both anti-tag and anti-NSP5 (data not shown).

For further confirmation, we used other constructs in which enhanced green fluorescent protein (EGFP) was fused to different regions of NSP5 (Fig. 9A). Cells were cotransfected with the tag-VP1 and the different EGFP constructs and DSP cross-linked, and the lysates were immunoprecipitated with anti-tag antibody. While the EGFP protein fused with only region 1 was not coimmunoprecipitated with anti-tag antibody, the

fusion proteins containing regions 4 and T (amino acids 130 to 198), with or without region 1, were pulled down (Fig. 9C), confirming that the N terminus does not bind to VP1 and, more importantly, that the last 68 amino acids (4T) were sufficient for the interaction. Furthermore, coimmunoprecipitation of tag-VP1 with EGFP-4T was obtained with anti-NSP5 (Fig. 9C).

In order to better define the region involved, we analyzed another deletion mutant of NSP5, lacking the last 48 amino acids (ΔC48). In parallel, we tested mutants ΔT and Δ4ΔT as controls (see diagrams in Fig. 9A). After cotransfection with tag-VP1, the anti-tag antibody did not coimmunoprecipitate ΔC48, nor did anti-NSP5 tag-VP1 (Fig. 9D). Moreover, when supernatants of samples already immunoprecipitated with anti-tag were subsequently immunoprecipitated with anti-NSP5, the noninteracting mutants (ΔT, Δ4ΔT, and ΔC48) were detected, but not the interacting wild-type NSP5 (data not shown).

To rule out the possibility that the lack of interaction of mutant ΔC48 was the consequence of the removal of a series of basic residues (two arginines and seven lysines) that could have been involved in the cross-linking with DSP, we carried out immunoprecipitations with anti-tag, which does not require cross-linking and efficiently coimmunoprecipitates wild-type NSP5. As shown in Fig. 9E, anti-tag was completely unable to coimmunoprecipitate ΔC48 in conditions in which the wild type did. Taken together, the results shown in Fig. 9 indicate that the 48 amino acids of the C-terminal region of NSP5 are essential for interaction with VP1.

DISCUSSION

In this study we aimed at clarifying the interactions between the rotavirus RNA polymerase VP1 and the nonstructural proteins NSP5 and NSP2. These two proteins, which are well known to interact with each other within cytoplasmic viroplasms (1, 12, 17, 40), have been proposed to actively participate in the replication of the viral genomic RNA (4, 8, 44). NSP2, because of its ATPase activity, has been suggested to work as a molecular motor to recruit single-stranded RNA templates for the synthesis of the genomic dsRNA by the VP1/VP2 replication complex (43, 46).

The capacity of NSP5 to interact with VP1 and NSP2 in virus-infected cells has already been observed in coimmunoprecipitation assays from DSP-cross-linked extracts (1). Here we provide a more detailed description of the nature of the interaction of VP1 with NSP5, with NSP2, or with both in the absence of other viral proteins or "true" viral RNA (the viral proteins are translated from transcripts of plasmids containing only cDNA comprising the coding regions and lacking the 5′ and 3′ untranslated regions).

Using extracts of cotransfected MA104 cells, we show by coimmunoprecipitation assays that NSP5 has a strong interaction with VP1, which is not altered by the presence of NSP2. On the other hand, interaction of NSP2 with VP1 appears to be much weaker and is possibly stabilized by NSP5 (observed in DSP-cross-linked extracts). Although it was not formally proven, the formation of a ternary complex of VP1, NSP5, and NSP2 is a possibility, since tag-VP1 was found in the VLS formed as a consequence of the interaction of the two others (Fig. 6). An interaction between NSP2 and VP1 in rotavirus-infected cells has been reported previously (25). When VP1 was coexpressed with each of the nonstructural proteins individually, it became apparent that NSP5 interacted more strongly with VP1 than NSP2. However, when the three proteins were coexpressed, NSP5 seemed to enhance the interaction of VP1 with NSP2, a conclusion delineated by data using DSP-cross-linked extracts. Interestingly, several attempted pull-down experiments with anti-NSP2 serum did not coimmunoprecipitate NSP5 (as has already been published [(1]) or VP1. Thus, it is likely that most of the NSP2 molecules are buried within the cross-linked complex and therefore are not accessible to the precipitating antibody.

Using NSP5 deletion mutants, we found that deletion of the N-terminal 33-amino-acid region from NSP5 did not affect binding to VP1, while deletion of the last 18 amino acids from the C terminus substantially reduced the interaction, and that of the last 48 amino acids completely abolished it (Fig. 9). Also, results with single-domain EGFP fusion chimeras allowed us to identify the 48 amino acids at the C terminus as those involved in the interaction with VP1. Since the last 18 C-terminal amino acids of NSP5 have previously been found to be involved in dimerization (13, 48), our data suggest that dimeric NSP5 is better suited for interaction and that the binding region is located just upstream of the C-terminal tail. The region of VP1 interacting with NSP5 remains to be determined.

In some experiments, we used in vivo cross-linking with DSP to stabilize the complexes. This was needed in particular when using the anti-NSP5 serum, possibly because the high-affinity hyperimmune polyclonal antibody has a dissociating activity. By contrast, the anti-tag monoclonal antibody, which binds to the N terminus of tag-VP1, allowed efficient coimmunoprecipitation of NSP5 or NSP2 or both from extracts that have not been cross-linked (Fig. 7).

So far, NSP5 has been proposed to have a crucial structural role, together with NSP2, in the assembly of viroplasms (8, 30, 44, 51). However, from the results presented here, new possible functions are emerging. The strong interaction between NSP5 and VP1 suggests that NSP5 may act at the crossroad of important processes of virus morphogenesis, such as replication, carried out by VP1 in conjunction with the scaffold protein VP2 (35, 37, 54), and packaging, for which NSP2 is a putative molecular motor (46).

It has been reported that NSP5 interacts with VP2 (5). We observed that NSP5 and VP2, either when coexpressed after transfection or in infected cells, were unable to coimmunoprecipitate from extracts, which had been cross-linked with DSP or not cross-linked. In spite of this lack of interaction, NSP5 hyperphosphorylation was considerably increased in the presence of VP2. This is a novel finding requiring further analysis.

In cotransfected cells, the presence of VP1 impaired the recognized ability of NSP2 to up-regulate NSP5 phosphorylation (1), but in spite of this, interaction between VP1 and NSP5 was not altered. Further data for virus-infected cells indicate that this interaction is independent of the phosphorylation status of NSP5 (M. Campagna et al., unpublished data). While this is an interesting observation, at present there are insufficient data for a comprehensive interpretation of whether and

how NSP5 hyperphosphorylation is linked to replication and packaging.

Some of the results of this work were obtained by using a VP1 derivative in which the 11-amino-acid-long SV5 tag was fused to the N terminus of VP1. The presence of a terminal tag allowed VP1 to be recognized by using immunoprecipitation or immunofluorescence assays. It also allowed us to overcome the problem of having only a poorly reactive antibody against the wild-type protein. The polyclonal antiserum against VP1 did not react in either immunoprecipitation or immunofluorescence experiments, but only in Western blots. It is possible that the antibody, which was made against the N-terminal 435 amino acids, did not recognize the folded full-length VP1 protein, while it was able to react with the denatured protein in Western blots. By contrast, the availability of a potent anti-tag monoclonal antibody allowed the interaction of VP1 with NSP5 and NSP2 to be studied. In doing so, it had to be considered that fusing tags to a protein may modify its structural and functional properties and may lead to artifacts and misinterpretations (7). Therefore, in order to ensure the validity of using a tagged version of VP1, we analyzed the behavior of such a protein in the context of viral infection by using immunofluorescence and analysis of purified viral particles. We found that tag-VP1 was localized in viroplasms and VLS (Fig. 5 and 6) and also packaged into viral progeny (Fig. 4). The incorporation efficiency was not high but was unequivocal and reproducible. Thus, only a few among the 12 molecules of the VP1 polymerase per viral particle (41) would be represented by the tagged VP1. The degree of tag-VP1 packaging varied, possibly depending on the relative ratios of infectious units of vaccinia virus and rotavirus, as well as on differences in the maturation of DLPs into TLPs. Nonspecific attachment of tag-VP1 to TLPs was ruled out by EDTA treatment of TLPs, which did not remove tag-VP1, and also by mixing TLPs with extracts containing an excess of tag-VP1, not leading to an association of these two components (results not shown).

Success in packaging tag-VP1 strengthens the results obtained in this work and represents a technical novelty. The system mainly used so far to study interactions among the structural proteins and their role in rotavirus morphogenesis (9, 10, 27, 42) is based on the coexpression of various combinations of structural proteins or derivatives thereof from baculovirus vectors in insect cells, forming so-called virus-like-particles. Although virus-like-particles have the structural characteristics and some of the functional properties of rotavirus particles (54), their assembly occurs outside the context of natural infection. The data provided here demonstrate that the incorporation of the exogenous protein into viral particles can take place during natural infection, indicating new possibilities for studying viral morphogenesis. While the improvement of an already developed reverse genetics system (26) and the development of new ones are under investigation, inserting recombinant proteins into progeny particles during natural viral infection could help to further define the roles of viral proteins.

ACKNOWLEDGMENTS

A gift of VP2-specific polyclonal guinea pig antiserum from John Patton is gratefully acknowledged.

F.A. was supported by an ICGEB predoctoral fellowship of the Corso di Perfezionamento of the Scuola Normale Superiore di Pisa.

REFERENCES

1. **Afrikanova, I., E. Fabbretti, M. C. Miozzo, and O. R. Burrone.** 1998. Rotavirus NSP5 phosphorylation is up-regulated by interaction with NSP2. J. Gen. Virol. **79:**2679–2686.
2. **Afrikanova, I., M. C. Miozzo, S. Giambiagi, and O. Burrone.** 1996. Phosphorylation generates different forms of rotavirus NSP5. J. Gen. Virol. **77:** 2059–2065.
3. **Aponte, C., D. Poncet, and J. Cohen.** 1996. Recovery and characterization of a replicase complex in rotavirus-infected cells by using a monoclonal antibody against NSP2. J. Virol. **70:**985–991.
4. **Arias, C. F., M. A. Dector, L. Segovia, T. Lopez, M. Camacho, P. Isa, R. Espinosa, and S. Lopez.** 2004. RNA silencing of rotavirus gene expression. Virus Res. **102:**43–51.
5. **Berois, M., C. Sapin, I. Erk, D. Poncet, and J. Cohen.** 2003. Rotavirus nonstructural protein NSP5 interacts with major core protein VP2. J. Virol. **77:**1757–1763.
6. **Blackhall, J., A. Fuentes, K. Hansen, and G. Magnusson.** 1997. Serine protein kinase activity associated with rotavirus phosphoprotein NSP5. J. Virol. **71:**138–144.
7. **Campagna, M., and O. R. Burrone.** 2006. Fusion of tags induces spurious phosphorylation of rotavirus NSP5. J. Virol. **80:**8283–8284; author reply, 8284–8285.
8. **Campagna, M., C. Eichwald, F. Vascotto, and O. R. Burrone.** 2005. RNA interference of rotavirus segment 11 mRNA reveals the essential role of NSP5 in the virus replicative cycle. J. Gen. Virol. **86:**1481–1487.
9. **Charpilienne, A., M. Nejmeddine, M. Berois, N. Parez, E. Neumann, E. Hewat, G. Trugnan, and J. Cohen.** 2001. Individual rotavirus-like particles containing 120 molecules of fluorescent protein are visible in living cells. J. Biol. Chem. **276:**29361–29367.
10. **Crawford, S. E., M. Labbé, J. Cohen, M. H. Burroughs, Y. J. Zhou, and M. K. Estes.** 1994. Characterization of virus-like particles produced by the expression of rotavirus capsid proteins in insect cells. J. Virol. **68:**5945–5952.
11. **Eichwald, C., G. Jacob, B. Muszynski, J. E. Allende, and O. R. Burrone.** 2004. Uncoupling substrate and activation functions of rotavirus NSP5: phosphorylation of Ser-67 by casein kinase 1 is essential for hyperphosphorylation. Proc. Natl. Acad. Sci. USA **101:**16304–16309.
12. **Eichwald, C., J. F. Rodriguez, and O. R. Burrone.** 2004. Characterization of rotavirus NSP2/NSP5 interactions and the dynamics of viroplasm formation. J. Gen. Virol. **85:**625–634.
13. **Eichwald, C., F. Vascotto, E. Fabbretti, and O. R. Burrone.** 2002. Rotavirus NSP5: mapping phosphorylation sites and kinase activation and viroplasm localization domains. J. Virol. **76:**3461–3470.
14. **Estes, M. K.** 2001. Rotaviruses and their replication, p. 1747–1785.1 *In* D. M. Knipe, P. M. Howley, D. E. Griffin, R. A. Lamb, M. A. Martin, B. Roizman, and S. E. Straus (ed.), Fields virology, 4th ed. Lippincott Williams & Wilkins, Philadelphia, PA.
15. **Estes, M. K., D. Y. Graham, C. P. Gerba, and E. M. Smith.** 1979. Simian rotavirus SA11 replication in cell cultures. J. Virol. **31:**810–815.
16. **Estes, M. K., D. Y. Graham, E. M. Smith, and C. P. Gerba.** 1979. Rotavirus stability and inactivation. J. Gen. Virol. **43:**403–409.
17. **Fabbretti, E., I. Afrikanova, F. Vascotto, and O. R. Burrone.** 1999. Two non-structural rotavirus proteins, NSP2 and NSP5, form viroplasm-like structures in vivo. J. Gen. Virol. **80:**333–339.
18. **Fuerst, T. R., E. G. Niles, F. W. Studier, and B. Moss.** 1986. Eukaryotic transient-expression system based on recombinant vaccinia virus that synthesizes bacteriophage T7 RNA polymerase. Proc. Natl. Acad. Sci. USA **83:**8122–8126.
19. **Gallegos, C. O., and J. T. Patton.** 1989. Characterization of rotavirus replication intermediates: a model for the assembly of single-shelled particles. Virology **172:**616–627.
20. **Glass, R. I., J. S. Bresee, U. Parashar, M. Miller, and J. R. Gentsch.** 1997. Rotavirus vaccines at the threshold. Nat. Med. **3:**1324–1325.
21. **Glass, R. I., J. S. Bresee, U. D. Parashar, B. Jiang, and J. Gentsch.** 2004. The future of rotavirus vaccines: a major setback leads to new opportunities. Lancet **363:**1547–1550.
22. **González, S. A., and O. R. Burrone.** 1991. Rotavirus NS26 is modified by addition of single O-linked residues of N-acetylglucosamine. Virology **182:** 8–16.
23. **Graham, A., G. Kudesia, A. M. Allen, and U. Desselberger.** 1987. Reassortment of human rotavirus possessing genome rearrangements with bovine rotavirus: evidence for host cell selection. J. Gen. Virol. **68:**115–122.
24. **Jiang, X., H. Jayaram, M. Kumar, S. J. Ludtke, M. K. Estes, and B. V. Prasad.** 2006. Cryoelectron microscopy structures of rotavirus NSP2-NSP5 and NSP2-RNA complexes: implications for genome replication. J. Virol. **80:**10829–10835.
25. **Kattoura, M. D., X. Chen, and J. T. Patton.** 1994. The rotavirus RNA-binding protein NS35 (NSP2) forms 10S multimers and interacts with the viral RNA polymerase. Virology **202:**803–813.
26. **Komoto, S., J. Sasaki, and K. Taniguchi.** 2006. Reverse genetics system for

introduction of site-specific mutations into the double-stranded RNA genome of infectious rotavirus. Proc. Natl. Acad. Sci. USA **103:**4646–4651.
27. **Labbé, M., A. Charpilienne, S. E. Crawford, M. K. Estes, and J. Cohen.** 1991. Expression of rotavirus VP2 produces empty corelike particles. J. Virol. **65:**2946–2952.
28. **Laemmli, U. K.** 1970. Cleavage of structural proteins during the assembly of the head of bacteriophage T4. Nature **227:**680–685.
29. **Lawton, J. A., C. Q. Zeng, S. K. Mukherjee, J. Cohen, M. K. Estes, and B. V. Prasad.** 1997. Three-dimensional structural analysis of recombinant rotavirus-like particles with intact and amino-terminal-deleted VP2: implications for the architecture of the VP2 capsid layer. J. Virol. **71:**7353–7360.
30. **López, T., M. Rojas, C. Ayala-Breton, S. Lopez, and C. F. Arias.** 2005. Reduced expression of the rotavirus NSP5 gene has a pleiotropic effect on virus replication. J. Gen. Virol. **86:**1609–1617.
31. **Mitchell, D. B., and G. W. Both.** 1990. Completion of the genomic sequence of the simian rotavirus SA11: nucleotide sequences of segments 1, 2, and 3. Virology **177:**324–331.
32. **Mohan, K. V., J. Muller, I. Som, and C. D. Atreya.** 2003. The N- and C-terminal regions of rotavirus NSP5 are the critical determinants for the formation of viroplasm-like structures independent of NSP2. J. Virol. **77:** 12184–12192.
33. **Parashar, U. D., E. G. Hummelman, J. S. Bresee, M. A. Miller, and R. I. Glass.** 2003. Global illness and deaths caused by rotavirus disease in children. Emerg. Infect. Dis. **9:**565–572.
34. **Patton, J., V. Chizhikov, Z. Taraporewala, and D. Y. Chen.** 2000. Virus replication, p. 33–66. *In* J. Gray and U. Desselberger (ed.), Rotaviruses: methods and protocols. Humana Press, Totowa, NJ.
35. **Patton, J. T.** 1996. Rotavirus VP1 alone specifically binds to the 3′ end of viral mRNA, but the interaction is not sufficient to initiate minus-strand synthesis. J. Virol. **70:**7940–7947.
36. **Patton, J. T., and C. O. Gallegos.** 1988. Structure and protein composition of the rotavirus replicase particle. Virology **166:**358–365.
37. **Patton, J. T., M. T. Jones, A. N. Kalbach, Y. W. He, and J. Xiaobo.** 1997. Rotavirus RNA polymerase requires the core shell protein to synthesize the double-stranded RNA genome. J. Virol. **71:**9618–9626.
38. **Petrie, B. L., D. Y. Graham, H. Hanssen, and M. K. Estes.** 1982. Localization of rotavirus antigens in infected cells by ultrastructural immunocytochemistry. J. Gen. Virol. **63:**457–467.
39. **Petrie, B. L., H. B. Greenberg, D. Y. Graham, and M. K. Estes.** 1984. Ultrastructural localization of rotavirus antigens using colloidal gold. Virus Res. **1:**133–152.
40. **Poncet, D., P. Lindenbaum, R. L'Haridon, and J. Cohen.** 1997. In vivo and in vitro phosphorylation of rotavirus NSP5 correlates with its localization in viroplasms. J. Virol. **71:**34–41.
41. **Prasad, B. V., R. Rothnagel, C. Q. Zeng, J. Jakana, J. A. Lawton, W. Chiu, and M. K. Estes.** 1996. Visualization of ordered genomic RNA and localization of transcriptional complexes in rotavirus. Nature **382:**471–473.
42. **Sabara, M., M. Parker, P. Aha, C. Cosco, E. Gibbons, S. Parsons, and L. A. Babiuk.** 1991. Assembly of double-shelled rotaviruslike particles by simultaneous expression of recombinant VP6 and VP7 proteins. J. Virol. **65:**6994–6997.
43. **Schuck, P., Z. Taraporewala, P. McPhie, and J. T. Patton.** 2001. Rotavirus nonstructural protein NSP2 self-assembles into octamers that undergo ligand-induced conformational changes. J. Biol. Chem. **276:**9679–9687.
44. **Silvestri, L. S., Z. F. Taraporewala, and J. T. Patton.** 2004. Rotavirus replication: plus-sense templates for double-stranded RNA synthesis are made in viroplasms. J. Virol. **78:**7763–7774.
45. **Southern, J. A., D. F. Young, F. Heaney, W. K. Baumgartner, and R. E. Randall.** 1991. Identification of an epitope on the P and V proteins of simian virus 5 that distinguishes between two isolates with different biological characteristics. J. Gen. Virol. **72:**1551–1557.
46. **Taraporewala, Z., D. Chen, and J. T. Patton.** 1999. Multimers formed by the rotavirus nonstructural protein NSP2 bind to RNA and have nucleoside triphosphatase activity. J. Virol. **73:**9934–9943.
47. **Taraporewala, Z. F., and J. T. Patton.** 2001. Identification and characterization of the helix-destabilizing activity of rotavirus nonstructural protein NSP2. J. Virol. **75:**4519–4527.
48. **Torres-Vega, M. A., R. A. Gonzalez, M. Duarte, D. Poncet, S. Lopez, and C. F. Arias.** 2000. The C-terminal domain of rotavirus NSP5 is essential for its multimerization, hyperphosphorylation and interaction with NSP6. J. Gen. Virol. **81:**821–830.
49. **Towbin, H., T. Staehelin, and J. Gordon.** 1979. Electrophoretic transfer of proteins from polyacrylamide gels to nitrocellulose sheets: procedure and some applications. Proc. Natl. Acad. Sci. USA **76:**4350–4354.
50. **Valenzuela, S., J. Pizarro, A. M. Sandino, M. Vasquez, J. Fernandez, O. Hernandez, J. Patton, and E. Spencer.** 1991. Photoaffinity labeling of rotavirus VP1 with 8-azido-ATP: identification of the viral RNA polymerase. J. Virol. **65:**3964–3967.
51. **Vascotto, F., M. Campagna, M. Visintin, A. Cattaneo, and O. R. Burrone.** 2004. Effects of intrabodies specific for rotavirus NSP5 during the virus replicative cycle. J. Gen. Virol. **85:**3285–3290.
52. **Vende, P., Z. F. Taraporewala, and J. T. Patton.** 2002. RNA-binding activity of the rotavirus phosphoprotein NSP5 includes affinity for double-stranded RNA. J. Virol. **76:**5291–5299.
53. **Welch, S. K., S. E. Crawford, and M. K. Estes.** 1989. Rotavirus SA11 genome segment 11 protein is a nonstructural phosphoprotein. J. Virol. **63:**3974–3982.
54. **Zeng, C. Q., M. J. Wentz, J. Cohen, M. K. Estes, and R. F. Ramig.** 1996. Characterization and replicase activity of double-layered and single-layered rotavirus-like particles expressed from baculovirus recombinants. J. Virol. **70:**2736–2742.